Research Article

Journal of Applied Material Science & Engineering Research

# Effect of on the Membrane Distillation of PVDF Membrane Material Enhanced by Gas-Liquid Two-Phase Flow

**Dashuai Zhang[1,2], Xiaopeng Zhang[1,2], YuqinXiong[1,2], Di Wu[1,2], ZaifengShi[1,2*], QiangLin[1,2], Fan Zhou[1], Fei Gao[1],Lixin Zhou[1], Xueying Cheng[1], Yunjuan Pu[1]**

*[1]Key Laboratory of Water Pollution Treatment & Resource Reuse, Hainan Normal University, Haikou, Hainan 571158, P.R. China*

*[2]College of Chemistry and Chemical Engineering, Hainan Normal University, Haikou, Hainan 571158, P.R. China*

**[*]Corresponding author**

Zaifeng Shi, Environmental chemistry, Key Laboratory of Water Pollution Treatment & Resource Reuse, Hainan Normal University, Haikou, Hainan 571158, P.R. China, Tel: +86 13086013920; E-mail: zaifengshi@163.com

**Submitted**: 27 Feb 2018; **Accepted**: 06 Mar 2018; **Published**: 20 Mar 2018

## Abstract

*This study investigates the membrane performance and fouling control in the bubble-assisted sweeping gas membrane distillation with high concentration saline (333 K saturated solution) as feed. The results show that longer bubbling interval (3 min) at a fixed bubbling duration of 30 s can most efficiently increase the flux enhancement ratio up to 1.518. Next, the flux increases with the gas flow rate under a relatively lower level, but tends to a plateau after the threshold level (1.2 L•min$^{-1}$). Compared to non-bubbling case, the permeate flux reaches up to 1.623 fold at a higher bubble relative humidity of 80 %. It was also found that greater flux enhancement can be achieved and meanwhile dramatic flux decline can be delayed for an intermittent bubbling system with a smaller nozzle size. These results accord well with the observations of fouling deposition in situ on the membrane surface with SEM.*

**Keywords:** Membrane Distillation, Gas-Liquid Two-Phase Flow, High Concentration Saline, Fouling Control

## Introduction

Membrane distillation (MD) is an innovative separation technology for desalination, and water & wastewater treatment due to its merits of mild operation temperature and pressure, with appropriate penetration rate, high rejection rate for nonvolatile components and small footprint when consuming alternative energy sources (e.g. low-grade thermal energy or waste heat) [1-8]. Unlike pressure-driven membrane processes such as reverse osmosis (RO), nanofiltration (NF), ultrafiltration (UF), microfiltration (MF), MD is an emerging thermally-driven technology coupled with mass and heat transfer process. Thereby, MD is an appealing method for extra-high concentration brine treatment owing to its insensitivity to feed salinity [9-13].

However, the decrease of driving force due to concentration and temperature polarization effects as well as fouling/scaling issues impedes the long-term stability performance of MD [14-16]. In MD process, inorganic fouling (scaling), organic fouling and biological fouling (biofouling) can be found according to contaminated material [17-20]. Many optimization strategies have been adopted to minimize the extent of fouling: (a) pretreatment, (b) membrane flushing, (c) gas bubbling, (d) temperature and flow reversal, (e) surface modification for anti-fouling membrane, (f) effect of magnetic/ ultrasonic field, (g) use of anticalants, (h) chemical cleaning [20-27].

As one of the most promising flux enhancement and anti-fouling techniques, the gas-liquid two-phase flow can induce secondary flow to maximize the shear stress at the membrane surface, displace the concentration and temperature layer, cause pressure pulsing and increase superficial cross-flow velocity [28-29]. Gas sparging technology has been successfully applied to traditional membrane separation technologies (MST) such as MF, UF and membrane bioreactors (MBRs) [30-32]. In recent years, there is a keen interest on MD process enhanced by gas-liquid two-phase flow for general desalination applications. For instance, Ding et al. observed that the cleaning efficiency of gas bubbling is improved with the increase of gas flow rate and gas bubbling duration, and the decrease of membrane distillation when introducing intermittent gas bubbling during the concentration of traditional Chinese medicine (TCM) by direct contact membrane distillation (DCMD) Chen et al. achieved 26% permeation flux enhancement and later appearance of major flux decline by incorporating gas bubbling into DCMD when salt solution was concentrated from 18% to saturation. Also, it was found that heat-transfer coefficient and temperature polarization coefficient (TPC) reached up to 2.30- and 2.13-fold in comparison with non-bubbling DCMD [33-34]. A recent air-bubbling vacuum membrane distillation (AVMD) study proposed that the flux was doubled at certain feed velocity and gas/liquid proportion [36].

As an extension of intermittent bubble-enhanced MD process, this paper aims to research the bubble characteristics (i.e. bubble velocity, bubble relative humidity) and nozzle size on mass transfer intensification and scaling mitigation for supersaturated saline

solution as feed. Meanwhile, the anti-fouling efficiency in MD brine processing with gas-liquid two-phase can be achieved through the evaluation of the local fouling status on the membrane surface.

## Materials and Methods

### Materials and Membrane Module

A hollow-fiber hydrophobic MD membrane (Jack Co. Ltd., China) was employed in our bubble-assisted sweeping gas membrane distillation (SGMD) experiments. Each membrane is made of polyvinylidene fluoride (PVDF) with 78% porosity, 113±1.7° contact angle, 3.07 N breaking strength, 4.038 bar LEPw, 0.22 μm mean pore size, and its inner and outer diameter are 1.2 mm and 0.9 mm, respectively. All data on membrane properties were provided by the manufacturer.

Twenty fibers were emplaced in parallel in a transparent polypropylene (PC) housing of 230 mm length and 20 mm external surface diameter. The effective fiber length and membrane area in the module are 180 mm and ~ $1.526 \times 10^{-2}$ $m^2$ separately.

**Experimental Set-up** The experimental set-up is shown schematically in Fig. 1. The bubble-assisted SGMD system can be divided into two parts: thermal cycle (red flowline) and cooling cycle (blue flowline).

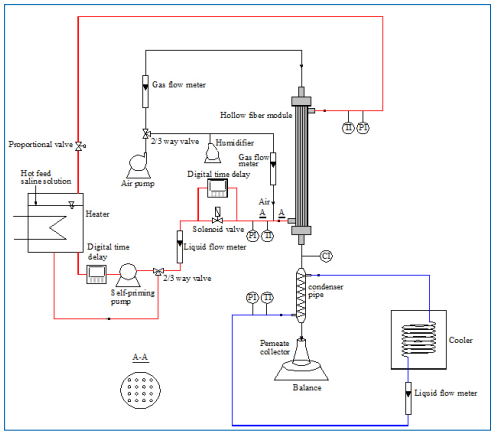


**Figure 1**: Diagramof experimental for bubble-assisted SGMD process.

In the thermal cycle, the hot feed maintained by a heater at constant temperature was circulated by a self-priming pump. The discharge pressure is manually adjusted by means of a 2/3 way valve on the pump's loop line. The bubble flow introduced by a air pump joins the feed flow at the entrance of membrane module, and therefore a gas-liquid two-phase flow is injected vertically upward into the membrane module. The velocity and relative humidity (RH) of bubble are controlled by gas flow meter and humidifier, respectively. The velocity, temperature and pressure and of feed were individually monitored by temperature indicator (TI), pressure indicator (PI) and rotameter.

In the cooling cycle, condensation water prepared from a cooler is recycled into the condenser pipe. Water vapor turns into water droplets when swept straightly down to condenser pipe by air pump. The weight and conductivity of penetrant are measured by a balance and conductivity indicator (CI), respectively.

The air pump not only acts as an aid to sweep gas into the membrane module, moreover it also supplies gas bubbling into the feed side. The bubble nozzle mounted at the feed side entrance of membrane module is used for dispersion of bubble.

### Experimental Part

In a bubbling system, bubble characteristic is a significant factor for the enhancement process. A series of experiments are conducted to research bubble on/off ratio (30 s/1 min, 30 s/2 min, 30 s/3 min), bubble flow rate ($Q_b$) (0 L/min, 0.4 L/min, 0.8 L/min, 1.2 L/min,, 1.6 L/min, 2 L/min), and bubble relative humidity ($RH_b$) (56%, 62%, 68%, 74%, 80%) on the flux enhancement when treated with saturated NaCl solution (333 K) as feed in bubble-assisted SGMD process.

Experiments are also carried out to investigate the effect of different nozzle sizes on the enhancement of critical flux and membrane fouling control. Nozzles with diameter ($D_n$) of 0 mm, 2.2 mm, 3.5 mm, 6.0mm and 10.0 mm are employed to produce bubbles.

All the above experiments were performed under Te same operating conditions: feed flow rate ($Q_f$) is 50 $L \cdot h^{-1}$, feed inlet temperature ($T_{f\text{-}in}$) on the shell side is 333 K, coolant temperature ($T_c$) is 283 K, gas-sweeping flow rate ($Q_a$) on the lumen side is 0.84 $m^3 \cdot h^{-1}$, and fill factor ($FF$) is 25.6%. Furthermore, indoor temperature and relative humidity are maintained constant at 26% and 74% respectively to reduce experimental error.

As for experiments of crystal deposition, each set of experiment was run with new membrane module during a specific time. After the membrane fouling experiment, the membrane module is removed from the apparatus immediately and then put into the constant-temperature oven for drying for 24 h at 303 K. The fouled fibers are cut off the head and tail, and taken the middle section to investigate the status of pollution situation by Scanning Electron Microscope (SEM).

For the recovery of membrane permeability, routine membrane cleaning was carried out after each bubble-enhanced SGMD experiment without crystal deposition, and the membranes were washed by the following procedure: (1) 30 min acid cleaning with 0.5 wt. % citric acid solution; (2) 1 h flushing by DI water.

## Results and Discussions

### Influence of bubble characteristics on mass transfer

### Bubble on/off ratio

Fig. 2 presents the comparison of trans-membrane flux enhancement ratio ($\Phi$) obtained by different flow regimes: single-phase flow, continuous gas-liquid two-phase flow, intermittent gas-liquid two-phase flow with three bubble on/off ratios (30 s/1 min, 30 s/2 min, 30 s/3 min). The other operating parameters are kept constant. All experiments last for 1 h.

In general, the histogram illustrates that the flux of bubbling case is above that of the non-bubbling case. The flux enhancement may be attributed to secondary flow by the introduction of bubble, which promotes the local mixing and increases the superficial cross-flow velocity. Consequently, the temperature/concentration layer at the membrane surface is reduced, and then a higher flux is obtained in a bubbling SGMD process.

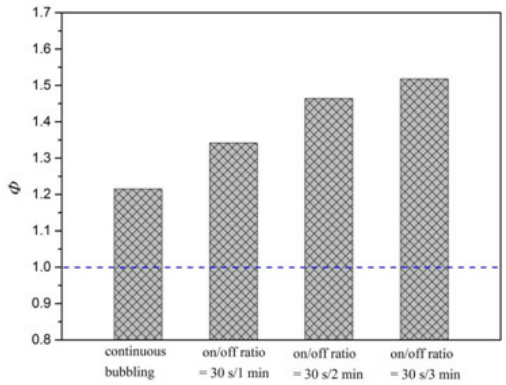


**Figure 2**: Effect of continuous and intermittent gas bubbling on trans-membrane flux (333 K saturated NaCl solution as feed: $Q_f$ = 50 L •h$^{-1}$; $T_{f\text{-}in}$ = 333 K ; $T_c$ = 283 K ; $Q_a$ = 0.84 m$^3$•h$^{-1}$ ; $FF$ = 25.6%, $Q_g$ = 0.5 L•h$^{-1}$; $RH_g$ = 74%; $D_n$ = 10.0 mm).

Also, it is observed that $\Phi$ value of the intermittent bubbling is higher than that of the continuous bubbling. The reason may be due to the prolonged occupation membrane surface by continuous bubbles, which reduces the effective contact area of feed and membrane surface. Furthermore, some bubbles existing in the membrane pore passages may block the way of water vapor to the permeate side, resulting in a declining trans-membrane driving force. Additionally, $\Phi$ is increased from 1.215 to 1.518 with an increase in the bubbling interval from 1 to 3 min during a settled bubbling duration of 30 s. More feed passes through the module per unit time if the bubbling interval increases, i.e., the stranded bubbles can be duly taken away from the module with the aid of fluid. That makes the upward bubbles flow along the membrane surface together with the feed flow create moderate shear stress and feed mixing. Accordingly, a higher trans-membrane flux enhancement is got a longer at a longer bubble interval.

## Bubble flow Rate

A series of experiments with and without intermittent gas bubbling were conducted at relatively low feed flow rate (20, 30, 40, 50 L•h$^{-1}$) for 60-min experiment operation. During the intermittent bubbling experiments, the effect of different gas flow rate (0.4, 0.8, 1.2, 1.6, 2.0 L•min$^{-1}$) on permeate flux were investigated respectively. Experimental results are shown in Fig. 3.

Clearly, four $J$ curves follow the similar trend, i.e., the $J$ initially increases with increasing gas flow rate ($0 \leq Q_g \leq 1.2$ L•min$^{-1}$) and then reaches a plateau at higher gas flow rate ($1.2 < Qg \leq 2.0$ L•min$^{-1}$). The reason for the increase may be due to the improvement of mass/heat transfer process induced by bubble. With the local mixing and surface shear force intensified by bubbling, the thinner temperature/concentration boundary layer results in an increase of partial pressure gradient. Therefore, the permeation flux increases correspondingly. However, when the feed flow rate is fixed at 20, 30, 40, 50 L•h$^{-1}$ respectively, the flux keeps on a stationary value from 1.80 to 2.03 L•m-2•h$^{-1}$ at the gas flow rate range from1.2 to 2.0 L•min$^{-1}$. This may be because that the slugging flow blocks the interfiber flow paths leading to local by-passing and uneven flow distribution, which counteracts the flux enhancement due to the negligibly intensified surface shear rate under a higher gas flow rate. As a result, the gas flow rate has little effect on the flux if it is higher than 1.2 L•min$^{-1}$. Hence, there is an preferable gas flow rate for gas bubbling to achieve a higher enhancement in flux, and excessive increase of gas flow rate may damage mechanical properties of fibers and increase energy consumption.

Furthermore, Fig. 3 shows that the permeate flux increase with the increasing feed flow rate under the same gas flow rate. With the high Reynolds number ($Re$) caused by the increasing $Q_f$, a better turbulent effect appears to decrease the mass transfer coefficient and improve the hydrodynamics adjacent to the feed-side membrane surface, leading to the weaker temperature and concentration polarization phenomena. Consequently, relatively higher feed flow rate along is better to bubbles distribution over the membrane surface and facilitate flow disturbance, in which the thermal boundary layer in the feed side may be reduced effectively, and hence the higher flux enhancement is obtained.

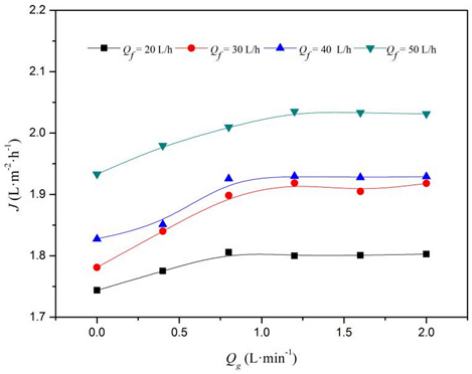


**Figure 3**: Effect of bubble flow rate on trans-membrane flux (333 K saturated NaCl solution as feed: $T_{f\text{-}in}$ = 333 K ; $T_c$ = 283 K ; $Q_a$ = 0.84 m$^3$•h$^{-1}$ ; $FF$ = 25.6%,

## Bubble Relative Humidity

The relationship between the flux enhancement ratio and the bubble relative humidity is plotted in Fig. 4. The 60-min experiment is run at a fixed parameters of $Q_g$ = 0.5 L•h$^{-1}$, $D_n$ = 10.0 mm, bubble on/off ratio = 30 s/3 min.

It can be seen that the $\Phi$ value increases dramatically from 1.228to 1.552at a range of $RH_g$ from 58% to 80%. As the bubble relative humidity increases, small bubbles are not vulnerable to explose and disappear and tend to aggregate into the formation of gaseous mass. Subsequently, gaseous mass flows with the feed flow in the hot feed side develop the slug flow (intermittent large bullet-shaped bubbles with less clear phase boundaries). The better turbulent effect is caused by the slug flow, and then the shear intensity at the membrane surface increases. Thereby, better membrane permeate performance can be attained in a relatively higher relative humidity.

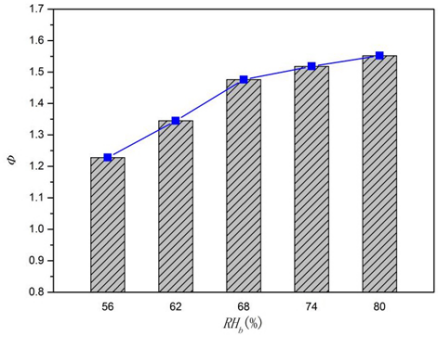


**Figure 4**: Effect of bubble relative humidity on trans-membrane

flux (333 K saturated NaCl solution as feed: $T_{f\text{-}in}$ = 333 K ; $T_c$ = 283 K ; $Q_a$ = 0.84 m$^3$•h$^{-1}$ ; $FF$ = 25.6%, $Q_g$ = 0.5 L•h$^{-1}$; $D_n$ = 10.0 mm; bubble on/off ratio = 30 s/3 min).

## Influence of nozzle size on bubble-assisted SGMD process

### The enhancement of critical flux

Fig. 5 shows the comparison of on the permeation flux vs. time with $D_n$ (0, 2.2, 3.5, 6.0, 10.0 mm) in intermittent bubble-assisted system. Saturated NaCl solution (333 K) is chosen as feed for 300 min in batch experiments.

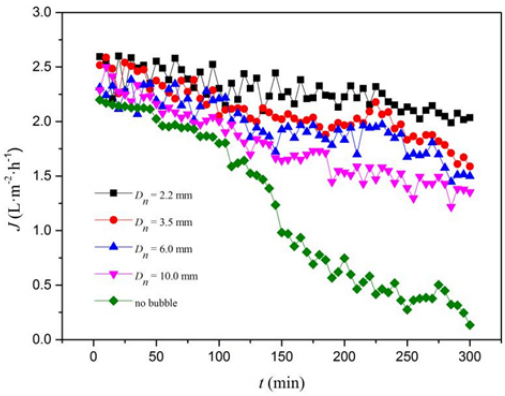


**Figure 5**: Effect of nozzle size on the enhancement of critical flux (333 K saturated NaCl solution as feed: $T_{f\text{-}in}$ = 333 K ; Tc = 283 K ; $Q_a$ = 0.84 m3•h$^{-1}$ ; $FF$ = 25.6%, $Q_g$ = 0.5 L•h$^{-1}$; $RH_g$ = 74%; bubble on/off ratio = 30 s/3 min).

As can be seen, the flux with two-phase flow is relatively larger than that with single flow throughout the experiments. Meanwhile, the permeate flux without injecting air in the feed stream decreases with time gradually. However, the fluxes maintain the relatively higher level at the beginning of the runs (0-110 min) with gas sparging. During 110-300 min, the flux is followed by a much slower decline with gas injection. At the point of 300 min, the flux drops essentially zero (~ 0.13 L•m$^{-2}$•h$^{-1}$) without bubbling. Unlike the sing-phase flow, the two-phase flow can not only promote local mixing near the membrane to displace upper part of the polarization layer , but also increase the feed side cross flow velocity, thus creating a better fluid hydrodynamics. Consequently, a flux increase contributes to the gas injection. The reason for sudden flux drop in the non-bubbling case may be that NaCl crystals accumulate on the membrane surface when the feed is concentrated to a critical hyper-saturated state with increasing operating time, thus increasing the thermal resistance (i.e., temperature drop) gradually. Consequently, a dramatic major decline occurrence follows.

For two-phase flow, it is clear that a smaller $D_n$ is helpful to attain a higher trans-membrane flux. The flux increases from ~ 1.35 to ~ 2.04 L•m$^{-2}$•h$^{-1}$with the declining $D_n$ from 10.0 to 2.2 cm at the end of the experimental operation. This may be because that larger bubble injected from the bigger nozzle results in local channeling (air bubble or bag blocking the flow of liquid in the channel) and uneven flow distribution. However, smaller bubbles induce the secondary flows and wakes, which enhances turbulence effect and the liquid convection. Additionally, the slug flow caused by smaller bubbles can form a annular falling film to create a high shear stress region. Therefore, it is necessary to identify the fine nozzle to avoid large bubble for bringing about superior evaporation performance in an incessant MD process.

## Scaling control

To further investigate the influence of gas bubbling with different $D_n$ on fouling control, the crystal deposition on the membrane surface is examined by SEM. Fig. 6. Shows SEM images of surfaces of membrane for six membrane systems: clean membrane, fouled membrane with gas-liquid two-phase flow ($D_n$ = 2.2, 3.5, 6.0, 10.0 mm), fouled membrane with single-phase flow.

In Fig. 6 (a), no crystal deposition is observed on the membrane surface for the fresh membrane. After 5-h operation, the membrane surface is almost completely covered with NaCl crystals for non-bubbling case; while a relatively small amount of crystals are observed for bubbling case. The physical observation of crystal deposition shows good agreement with the drastic flux decline presented in Fig. 5. With gas sparging, moving slugs cause pressure pulsing in the liquid around it, which disrupts the concentration polarization layer. Also, the enhanced sheer stress can peel the crystals adhere to the membrane surface. Therefore, fouling limitation is improved by gas bubbling at the feed side in SGMD.

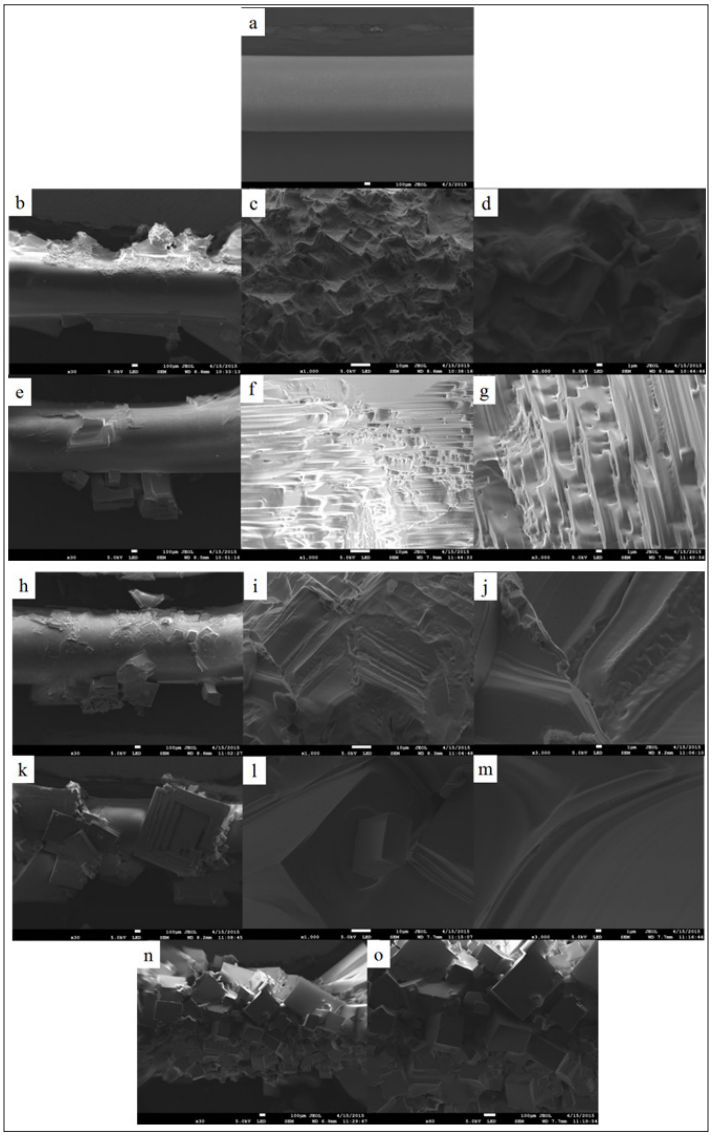


**Figure 6:** (a) SEM image of clean membrane (b-o) SEM images of fouled membrane in high concentration intermittent bubble-enhanced SGMD at different nozzle sizes: (b-d) $D_n$ = 2.2 mm; (e-g) $D_n$ = 3.5

mm; (h-j) $D_n$ = 6.0 mm; (k-m) Dn = 10.0

With the decrease of $D_n$, the fouling layer on the surface of membrane is much thinner. Additionally, the scaling deposition is close to less uniform cubic crystals and the crystal face is much rougher. This is consistent with of the tendency of flux decline with time. For smaller $D_n$ , more falling films and bubble wakes can be created the shear stress fluctuation in bubbling MD, which deters normal formation of NaCl crystals. Again, secondary flow induced by smaller bubbles is more helpful to erode the crystal attached on the membrane, leading to a uneven crystal surface. Hence, a gas sparging with smaller $D_n$ is confirmed to overcome the concentration polarization and mitigate the membrane fouling greatly.

## Conclusion

From this study, it was found that an intermittent gas flow seems to be more effective than a steady one in a same experimental operating, even if it improves the flux in comparison with the one without bubbling. A higher enhancement ratio (1.518) could be obtained with the bubble on/off ratio of 30 s/3 min. There is also an initial increase observed with the increase of gas flow rate. However, a further gas flow rate in permeate flux dose not result in any further improvement in the permeate flux. Besides, an reasonably high bubble relative humidity of 80 % is preferable for a higher flux enhancement ratio (1.623).

Experiments on a range of nozzle sizes have shown that, slugs in MD hollow fibers by gas-liquid two-phase flow are very efficient to enhance permeate flux when limited by crystal deposition. Smaller nozzle size is more useful to enhance permeate flux and postponed a sharp flux decline. The results are consistent with the inspection of membrane surface autopsy by SEM. It is observed that the less crystal deposition with rougher crystal face occurs on the membrane surface when using the smaller nozzle size (2.2 mm) in the intermittent gas bubbling experiment.

To sum it up, intermittent bubbling can not only improve the permeate flux, but also remove the deposited salt and foulants from the membrane surface. It is available to resist the fouling formation and deposition for high concentration SGMD process.


## Acknowledgment

Thanks are given to the Department of Science & Technology of Hainan Province, P.R.China for program fund (ZDKJ2016022, ZDYF2017011, 217100, 217101).


## References


1. Lawson KW, Lloyd DR (1996) Membrane distillation. I. Module design and performance evaluation using vacuum membrane distillation. J Membr Sci 120: 111-121.
2. Lawson KW, Lloyd DR (1997) Membrane distillation. J Membr Sci 124: 1-25.
3. Kubota S, Ohta K, Hayano I, Hirai M, Kikuchi K (1988) Experiments on seawater desalination by membrane distillation. Desal 69: 19-26.
4. EI-Bourawi MS, Ding Z, Ma R, Khayet M (2006) A framework for a better understanding membrane distillation separation process. J Membr Sci 285: 4-29.
5. Alkhudhiri A, Darwish N, Hilal N (2012) Membrane distillation: a comprehensive review. Desal 287: 2-18.
6. Banat F, Jumah R, Garaibeh M (2002) Exploitation of solar energy collected by solar stills for desalination by membrane distillation. Renew Energy 25: 293-305.
7. Schwantes R, Cipollina A, Gross F, Koschikowski J, Pfeifle D et al. (2013) Membrane distillation: Solar and waste heat driven demonstration plants for desalination. Desal 323: 93-106.
8. Jansen AE, Assink JW, Hanemaaijer JH, J van Medevoort, E van Sonsbeek (2013) Development and pilot testing of full-scale membrane distillation modules for deployment of waste heat. Desal 323: 55-65.
9. Alklaibi AM, Lior N (2005) Membrane-distillation desalination: status and potential. Desal 171: 111-131.
10. Yun YB, Ma RY, Zhang WZ, Fane AG, Li JD (2006) Direct contact membrane distillation mechanism for high concentration NaCl solutions. Desal 188: 251-262.
11. Martinetti CR, Childress AE, Cath TY (2009) High recovery of concentrated RO brines using forward osmosis and membrane distillation. J Membr Sci 331: 31-39.
12. Edwie F, Chung TS (2012) Development of hollow fiber membranes for water and salt recovery from highly concentrated brine via direct contact membrane distillation and crystallization J Membr Sci 422: 111-123.
13. Quist-Jensen CA, Ali A, Mondal S, Macedonio F, Drioli E (2016) A study of membrane distillation and crystallization for lithium recovery from high-concentration aqueous solutions J Membr Sci 505: 167-173.
14. R W Schofield, A G Fane, C J D Fell (1987) Heat and mass transfer in membrane distillation J Membr Sci 33: 299-313.
15. Martínez-Díez L, Vázquez-González MI (1996) Temperature and concentration polarization in membrane distillation of aqueous salt solutions J Membr Sci 156: 265-273.
16. Calabro V, Drioli E (1997) Polarization phenomena in integrated reverse osmosis and membrane distillation for seawater desalination and waste water treatment. Desal 108: 81-82.
17. Gryta M (2008) Alkaline scaling in the membrane distillation process. Desal 228: 128-134.
18. Gryta M, Tomaszewska M, Grzechulska J, Morawski AW (2001) Membrane distillation of NaCl solution containing natural organic matter. J Membr Sci 181: 279-287.
19. Krivorot M, Kushmaro A, Oren Y, Gilron J (2011) Factors affecting biofilm formation and biofouling in membrane distillation of seawater J Membr Sci 376: 15-24.
20. Tijing LD, Woo YC, Choi JS, Lee S, Kim SH et al. (2015) Fouling and its control in membrane distillation—A review. J Membr Sci 475: 215-244.
21. Ebrahim S, Abdel-Jawad M, Bou-Hamad S, Safar M (2001) Fifteen years of R&D program in seawater desalination at KISR Part I. Pretreatment technologies for RO systems. Desal 135: 141-153.
22. Nghiem LD, Cath T (2011) A scaling mitigation approach during direct contact membrane distillation. Purif Technol 80: 315-322.
23. Teoh MM, Bonyadi S, Chung TS (2008) Investigation of different hollow fiber module designs for flux enhancement in the membrane distillation process J Membr Sci 311: 371-379.
24. Hickenbottom KL, Cath TY (2014) Sustainable operation of membrane distillation for enhancement of mineral recovery from hyper saline solutions J Membr Sci 454: 426-435.
25. Xu JB, Lange S, Bartley JP, Johnson RA (2004) Alginate-coated microporous PTFE membrane for use in the osmotic distillation of oily feeds. J Membr Sci 240: 81-89.
26. Alimi F, Tlili M, Ben Amor M, Gabrielli C, Maurin G (2007) Influence of magnetic field on calcium carbonate precipitation.

Desal 206: 163-168.
27. Ghani S, Al-Deffeeri NS (2010) Impacts of different antiscalant dosing rates and their thermal performance in Multi Stage Flash (MSF) distiller in Kuwait Desal 250: 463-472.
28. Cui ZF, Chang S, Fane AG (2003) The use of gas bubbling to enhance membrane processes J Membr Sci 221: 1-35.
29. Wibisono Y, Cornelissen ER, Kemperman AJB, WGJ van der Meer, Nijmeijer K (2014) Two-phase flow in membrane process: A technology with a future J Membr Sci 453: 566-602.
30. Lu Y, Ding ZW, Liu LY, Wang ZJ, Ma RY (2008) The influence of bubble characteristics on the performance of submerged hollow fiber membrane module used in microfiltration Sci Technol 61: 89-95.
31. Tian JY, Xu YP, Chen ZL, Nan J, Li GB (2010) Air bubbling for alleviating membrane fouling of immersed hollow-fiber membrane for ultrafiltration of river water Desal 260: 225-230.
32. Cerón-Vivas A, Morgan-Sagastume JM, Noyola A (2012) Intermittent filtration and gas bubbling for fouling reduction in anaerobic membrane bioreactors, J. Membr. Sci 424: 136-142.
33. Ding ZW, Liu LY, Liu Z, Ma RY (2011) The use of intermittent gas bubbling to control membrane fouling in concentrating TCM extract by membrane distillation, J. Membr. Sci 372: 172-181.
34. Chen GZ, Yang X, Wang R, Fane AG (2013) Performance enhancement and scaling control with gas bubbling in direct contact membrane distillation Desal 308: 47-55.
35. Chen GZ, Yang X, Lu YH, Wang R, Fane AG (2014) Heat transfer intensification and scaling mitigation in bubbling-enhanced membrane distillation for brine concentration J Membr Sci 470: 60-69.
36. Wu CR, Li ZG, Zhang JH, Jia Y, Gao QJ et al. (2015) Study on the heat and mass transfer in air-bubbling enhanced vacuum membrane distillation Desal 373: 16-26.

**Copyright:** *©2018 Zaifeng Shi, et al. This is an open-access article distributed under the terms of the Creative Commons Attribution License, which permits unrestricted use, distribution, and reproduction in any medium, provided the original author and source are credited.*